

A complete electronic version of this article and other services, including high-resolution figures, can be found at:

<http://stm.sciencemag.org/content/2/15/15ra6.full.html>

Supporting Online Material can be found at:

"Supplementary Material"

<http://stm.sciencemag.org/content/suppl/2010/01/15/2.15.15ra6.DC1.html>

This article cites 25 articles, 13 of which can be accessed free:

<http://stm.sciencemag.org/content/2/15/15ra6.full.html#ref-list-1>

Information about obtaining reprints of this article or about obtaining permission to reproduce this article in whole or in part can be found at:

<http://www.sciencemag.org/about/permissions.dtl>

Identification of a Class of HCV Inhibitors Directed Against the Nonstructural Protein NS4B

Nam-Joon Cho,^{1,2} Hadas Dvory-Sobol,^{1*} Choongho Lee,^{1*} Sang-Joon Cho,³ Paul Bryson,¹ Marilyn Masek,¹ Menashe Elazar,¹ Curtis W. Frank,² Jeffrey S. Glenn^{1,4†}

(Published 20 January 2010; Volume 2 Issue 15 15ra6)

New classes of drugs are needed to combat hepatitis C virus (HCV), an important worldwide cause of liver disease. We describe an activity of a key domain, an amphipathic helix we termed 4BAH2, within a specific HCV nonstructural protein, NS4B. In addition to its proposed role in viral replication, we validate 4BAH2 as essential for HCV genome replication and identify first-generation small-molecule inhibitors of 4BAH2 that specifically prevent HCV replication within cells. Mechanistic studies reveal that the inhibitors target 4BAH2 function by preventing either 4BAH2 oligomerization or 4BAH2 membrane association. 4BAH2 inhibitors represent an additional class of compounds with potential to effectively treat HCV.

INTRODUCTION

Hepatitis C virus (HCV) is an important cause of worldwide chronic liver disease, infecting more than 150 million people (1). Current interferon and ribavirin treatment for HCV is quite toxic yet ineffective at curbing disease (2), highlighting the need for alternative therapies. Understanding of HCV molecular virology has led to the development of nonstructural protein 3 (NS3) protease and NS5B polymerase inhibitors (3). Although some of these agents have encouraging antiviral activity in vitro and in vivo, resistance to either of these classes of drugs develops rapidly, precluding their use as monotherapies. Hence, the identification of novel classes of drugs targeting multiple and independent virus-specific functions, similar to pharmacological cocktails used for tuberculosis and HIV, is imperative.

The 9.6-kb HCV genome is a positive single-stranded RNA that encodes for a 3010-amino acid protein (4). The immature protein is processed by cellular and viral proteases into structural components of the mature virus and nonstructural proteins that are involved in virus replication (5). All positive-strand RNA viruses replicate their genome in intimate association with host intracellular membranes (6–9). Some viruses, such as alphaviruses, exploit the surface of preexisting vesicular membranes like endosomes to replicate their genomes (10). Other viruses, such as HCV, induce the formation of novel membrane structures that facilitate their membrane-associated RNA replication (11). These membrane structures, termed the membranous web because of their appearance by electron microscopy, consist of aggregates of membrane vesicles and are believed to be derived in part from the endoplasmic reticulum (ER) (12, 13). One protein, NS4B, has been reported to be sufficient for creation of the membranous web (12, 13), although the molecular mechanism(s) whereby NS4B might promote membrane rearrangements or vesicle aggregations is largely unknown. NS4B has at least four predicted transmembrane domains (14–17). An N-terminal amphipathic helix within NS4B mediates the targeting of the HCV replicase complex components to the apparent sites of replication

(14), and an arginine-rich-like motif within NS4B binds the 3'-terminus region of the virus negative-strand RNA, the presumed template for the initiation of progeny plus-strand RNA genomes (18). Recently, we demonstrated that pharmacologic inhibitors of the NS4B RNA binding activity can be effective at inhibiting genome replication (18), but to date, no small molecules capable of inhibiting HCV amphipathic helix function within NS4B or other viral proteins have been identified.

Here, we validated an uncharacterized domain within NS4B that is essential for enabling genome replication. This target consists of a second amphipathic helix, termed 4BAH2, and was found to mediate NS4B oligomerization and lipid vesicle aggregation. The ability to induce vesicle aggregation also suggested a potential phenotypic readout for a high-throughput screen (HTS) to identify pharmacologic inhibitors of 4BAH2 function. We performed such a HTS and identified a variety of small molecules capable of inhibiting 4BAH2-mediated lipid vesicle aggregation and HCV RNA replication. Quartz crystal microbalance with dissipation (QCM-D) and atomic force microscopy (AFM) analyses of two of the compounds found to most potently inhibit vesicle aggregation revealed their mechanism of action on 4BAH2 function. These results highlight 4BAH2 as a critical modulator of NS4B function, provide new insight into the molecular mechanism of HCV replication platform assembly, and demonstrate the utility of a novel small-molecule anti-HCV strategy.

RESULTS

Amino acids 43 to 65 of NS4B constitute an amphipathic α helix (4BAH2)

Secondary structure prediction programs (including DSC, HNNC, MLRC, PHD, and Sec. Cons.) indicated that amino acids 43 to 65 of NS4B are likely to reside in an α -helical conformation (see fig. S1). Inspection of this helix revealed it to be amphipathic in nature (Fig. 1A). Because this segment is immediately downstream of another amphipathic helix (14), we defined the former as 4BAH2 and the proximal N-terminal amphipathic helix as 4BAH1 (14). Circular dichroism (CD) measurements confirmed the helical nature of a synthetic peptide corresponding to 4BAH2 (fig. S2) (19).

4BAH2 induces vesicle aggregation

Expression of NS4B has been reported to be necessary and sufficient for induction of the membranous web (12, 13). On the basis of initial

¹Division of Gastroenterology and Hepatology, School of Medicine, Stanford University, Stanford, CA 94305, USA. ²Department of Chemical Engineering, Stanford University, Stanford, CA 94305, USA. ³Park Systems Inc., Suwon 443-270, South Korea. ⁴Veterans Administration Medical Center, Palo Alto, CA 94304, USA.

*These authors contributed equally to this work.

†To whom correspondence should be addressed. E-mail: jeffrey.glenn@stanford.edu

pilot studies of the interaction of 4BAH2 with membrane constituents, we hypothesized that 4BAH2 might play a role in membranous web formation. To test this hypothesis, we studied the interaction of 4BAH2 with lipid vesicles composed of 1-palmitoyl-2-oleoyl-*sn*-glycero-3-phosphocholine (POPC). The POPC lipid was selected because phosphatidylcholine is the most abundant class of phospholipid in the ER. Dynamic light scattering (DLS) indicated that the extruded POPC vesicles had a relatively uniform size distribution (Fig. 1B). The average POPC vesicle diameter was 49.5 ± 1.4 nm and the relative variance (polydispersity) of the vesicles was 0.118 ± 0.02 nm. The 4BAH2 peptide was then added to the lipid vesicles, and the reaction was monitored by DLS. A large increase in the average size of the vesicle population was observed, whereas no such activity was observed with a control amphipathic helical peptide (4BAH1), highlighting the unique, specific, and striking biochemical activity associated with 4BAH2 (Fig. 1, C and D).

To determine whether the marked increase in size detected by DLS was due to vesicle fusion or vesicle aggregation, we performed transmission electron microscopy (TEM) on the vesicles before and after addition of 4BAH2 (Fig. 1, E and F). Most vesicles appeared to retain their initial size, indicating that they are predominantly organized into large aggregates upon addition of 4BAH2 (Fig. 1F). To further confirm this apparent 4BAH2-induced aggregation of lipid vesicles, we also used AFM to follow the morphological changes associated with the addition of 4BAH2 to lipid vesicles upon interaction with a solid support. We used the hydrophilic SiO₂ substrate (fig. S3A) because it is atomically flat and it is well known that vesicles typically fuse upon interaction with such hydrophilic substrates to make a bilayer ~ 5 nm thick (20). Upon addition of vesicles alone, the flat-appearing, uniform thickness of a ~ 4.5 -nm bilayer was observed (fig. S3B). As expected, upon deposition of vesicles in the presence of 4BAH2, we detected massive 4BAH2-induced vesicle aggregates (fig. S3C).

Disruption of 4BAH2's amphipathicity abrogates vesicle aggregation

To determine whether the amphipathic nature of 4BAH2 is necessary for its vesicle-aggregating activity, we generated 4BAH2 peptides (M2, M3, and M4) harboring two to four point mutations that introduced charged amino acids into the hydrophobic face of the 4BAH2 amphipathic helix (M2: A51E and W55D; M3: A51E, W55D, and I61D; M4: F49E, A51E, W55D, and I61D) (Fig. 2A) and tested their ability to mediate aggregation. Relative to wild-type 4BAH2 (Fig. 2C), point mutants M2, M3, and M4 that disrupted the amphipathic nature of 4BAH2 completely abrogated its vesicle-aggregating activity (Fig. 2, D to F). To confirm that these results were not due to conformational changes, we examined the ability of mutant 4BAH2 peptides to retain helicity and found that the loss of amphipathicity appeared to be a key determinant of the 4BAH2 mutants' inability to promote vesicle aggregation (Fig. 2G). Similar results were obtained with AFM (fig. S4). Moreover, the mutations did not appear to alter NS4B stability (fig. S5).

An intact 4BAH2 is required for HCV genome replication

To test the hypothesis that an intact 4BAH2 is essential for viral genome replication, we introduced the smallest number of mutations that were sufficient to abrogate 4BAH2's vesicle-aggregating activity (i.e., M2: A51E and W55D) into a bicistronic high-efficiency HCV replicon (21) modified so that the HCV internal ribosome entry site (IRES) drives the expression of luciferase, and the nonstructural proteins required for replication are expressed from the encephalomyocarditis

virus IRES. Transient replication assays were performed on wild-type, mutant, and negative control replicons harboring a lethal mutation of amino acids GDD to GND at codons 317 to 319 of NS5B (22). Disruption of 4BAH2 abrogated genome replication (Fig. 3A). To confirm the dependence of HCV replication on 4BAH2, we assayed analogous replicons, in which the luciferase gene was replaced with the neomycin phosphotransferase gene, in standard colony formation assays (Fig. 3B) (23). Wild-type replicons yielded numerous colonies, whereas no colonies resulted upon electroporation of the 4BAH2 mutant replicons (Fig. 3B). Together, these results demonstrate that mutations that impair the vesicle-aggregating activity of 4BAH2 abrogate HCV genome replication.

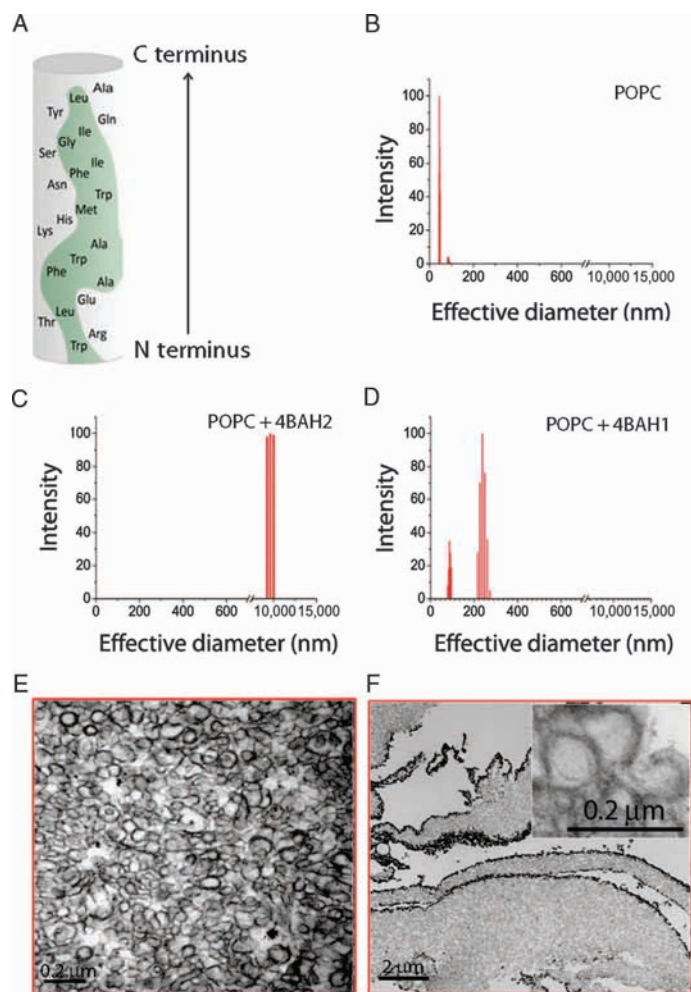


Fig. 1. An amphipathic α -helical segment of NS4B, 4BAH2, promotes large-scale vesicle aggregation. (A) Helix net diagram of amino acids 43 to 65 of NS4B that constitute 4BAH2 (depicted in the N-terminal to C-terminal direction from bottom to top). Hydrophobic portions are indicated in green. (B and C) Size distribution of lipid vesicles in the absence (B) or presence (C) of 4BAH2. (D) DLS of lipid vesicles with a control amphipathic helical peptide (4BAH1). The red bars represent the histogram of size distribution. Note that the x-axis scale is separated into two linear size ranges to directly compare the vesicle size distribution upon addition of wild-type 4BAH2 versus 4BAH1. (E and F) TEM images before (E) and after (F) addition of 4BAH2. Note that the inset image in the upper right corner of (F) has the same level of magnification as (E) for direct comparison.

Small molecules are identified that inhibit 4BAH2 activity

The above results validated the importance of 4BAH2 for HCV genome replication and elucidated a potential approach to identify pharmacologic inhibitors of 4BAH2 function. To do so, we fluorescently labeled POPC vesicles and monitored vesicle aggregation by fluorescence microscopy upon addition of 4BAH2. The assay was adapted to a 384-well format (fig. S6) and performed in the presence of compounds available from a small-molecule library (24). The presence or absence of aggregates was verified with pattern recognition software in a high-throughput scheme or by visual inspection (Fig. 4, A and B). Although most compounds had no significant effect on the vesicle-aggregating activity of 4BAH2, several inhibited aggregation formation to background levels observed without addition of 4BAH2. These candidate inhibitors, along with selected compounds that displayed no inhibition of lipid vesicle aggregation (negative controls), were further evaluated in a secondary screen in which DLS assays were performed in the presence of the individual compounds (Fig. 4C). Several of the candidate inhibitors were confirmed to be potent inhibitors of 4BAH2 lipid vesicle-aggregating activity, and we hypothesized that a subset of these, particularly C4 and A2, might similarly inhibit HCV genome replication.

Selected candidate inhibitors display genotype-specific effects on HCV replication

The importance of 4BAH2 to the HCV life cycle is indicated by several lines of genetic evidence. First, 4BAH2 is conserved across all HCV genotypes and isolates whose sequences are publicly available (fig. S7). Moreover, an HCV replicon harboring mutant 4BAH2 could not initiate genome replication (Fig. 3A) or sustain genome replication during colony formation (Fig. 3B). Thus, pharmacologic inhibition of 4BAH2 might be expected to inhibit HCV genome replication.

Transient replication assays using C4 and A2 (fig. S8) at low to submicromolar concentrations inhibited HCV replication in a dose-dependent manner (Fig. 5A). No significant cellular toxicity was observed under any of these conditions (Fig. 5B), highlighting the specificity of inhibition of HCV replication. The efficacy of C4 and A2 could be assessed on HCV clonal variants (genotypes 1b and 2a). We found that both compounds could inhibit genotype 1b (Fig. 5A), but only C4 inhibited genotype 2a replication (Fig. 5A). This suggests a difference in the specificity of the compounds for 4BAH2 on HCV clonal variants.

HCV variants did not impair the ability of 4BAH2 to induce vesicle aggregation (Fig. 5, C and D). Addition of either C4 or A2 inhibited vesicle aggregation induced by 4BAH2 of geno-

type 1b (Fig. 5C). However, only addition of C4, but not A2, abrogated the ability of 4BAH2 of genotype 2a to induce vesicle aggregation (Fig. 5D). These results parallel the inhibitory effects of the compounds on replication of the respective genotypes (Fig. 5A) and highlight the specificity of the two compounds for 4BAH2.

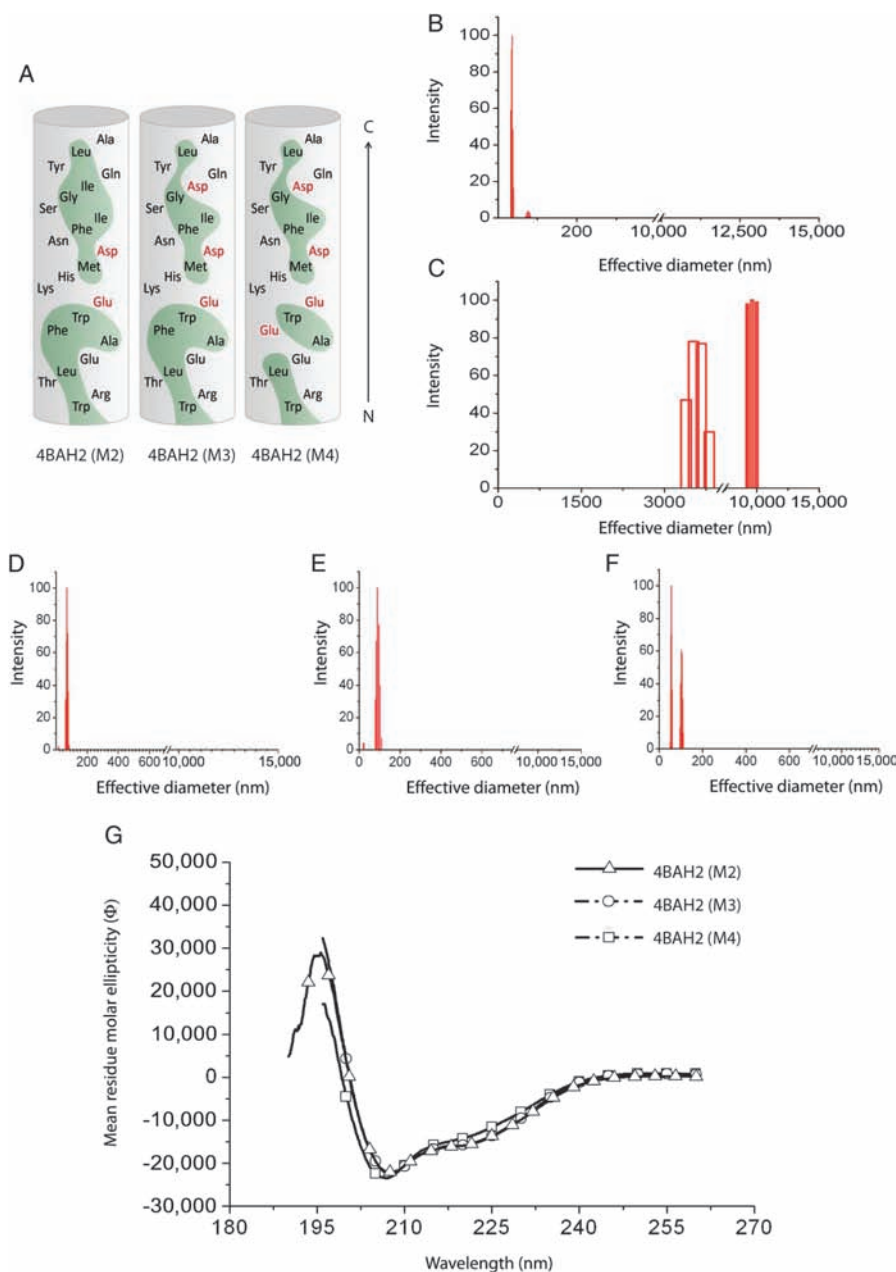


Fig. 2. Disruption of 4BAH2 amphipathicity abrogates vesicle aggregation. **(A)** Helix net diagrams (depicted in the N-terminal to C-terminal from bottom to top) of amino acids 43 to 65 of NS4B, which constitute 4BAH2, representing point mutations indicated in red. **(B to F)** POPC lipid vesicle size distribution was measured by DLS in the absence (B) or presence (C) of 4BAH2 or in the presence of mutant versions of 4BAH2 harboring (D) two point mutations, 4BAH2 (M2) (A51E and W55D), (E) three point mutations, 4BAH2 (M3) (A51E, W55D, and I61D), or (F) four point mutations, 4BAH2 (M4) (F49E, A51E, W55D, and I61D). Note that the x-axis scale is separated into two linear size ranges to directly compare the average vesicle size distribution on addition of the wild-type, but not mutant, 4BAH2 peptides. **(G)** Far-ultraviolet CD spectra of the 4BAH2 mutants.

A variety of mutations have been identified that confer phenotypic resistance to pharmacologic inhibition of 4BAH2. As expected, these mutations map to NS4B. Of note, A48Q, which is a single amino acid change within 4BAH2, increases the EC₅₀ (median effective concentration) for A2 by factors of 3 to 4 (fig. S9).

We envisage at least two possible mechanisms whereby 4BAH2-induced lipid vesicle aggregation can be inhibited: (i) preventing oligomerization of 4BAH2 peptides and/or (ii) disrupting the ability of 4BAH2 to interact with lipid vesicles (Fig. 6). To tease apart the mechanisms by which C4 and A2 compounds inhibited aggregation, we performed AFM to quantitatively determine surface topology and particle sizes of 4BAH2 oligomers (Fig. 7, A to D, and fig. S10) and QCM-D to assess membrane association (Fig. 7, E and F). The combined AFM and QCM-D data suggest that C4 acts primarily via disruption of 4BAH2 oligomerization (Fig. 7C), whereas the predominant effect of A2 is to prevent interaction of 4BAH2 with membranes (Fig. 7E). In particular, there is prominent self-oligomerization of 4BAH2 peptides in the absence of inhibitor (Fig. 7B), whereas self-oligomerization is dramatically inhibited in the presence of C4 (Fig. 7C). The extent of inhibition was as great as that achieved by mutations in 4BAH2 that blocked 4BAH2 oligomerization (fig. S11). In contrast, addition of A2 had a minimal effect on the ability of 4BAH2 to oligomerize (Fig. 7D) but completely prevented genotype 1b 4BAH2 membrane association (Fig. 7E and fig. S12). Again, the effect of A2 on 4BAH2 was limited to a genotype 1b target, with no significant inhibition of genotype 2a

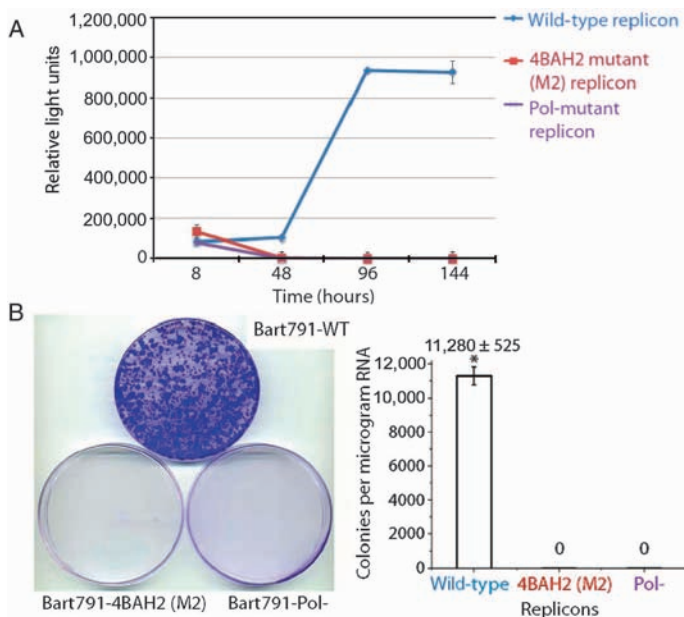


Fig. 3. An intact 4BAH2 domain of NS4B is required for HCV RNA genome replication. (A) Luciferase reporter-linked transient HCV replication assays were performed on Huh7 cells harboring wild-type (Bart791-luc-WT), 4BAH2 mutant [Bart791-luc-4B-AH2 (M2)], or negative control polymerase minus mutant (Bart791-luc-Pol-) luciferase harboring HCV replicon RNAs. (B) Colony formation assays of wild-type Huh7 cells harboring wild-type (Bart791-WT), 4BAH2 mutant [Bart791-NS4B-AH2 (M2)], or negative control polymerase minus mutant (Bart791-Pol-) HCV replicon RNAs containing the neomycin phosphotransferase gene. Surviving colonies were stained with crystal violet. Left panel, representative plates; right panel, average (±SD) number of colonies per microgram electroporated RNA (n = 3). *P < 0.01.

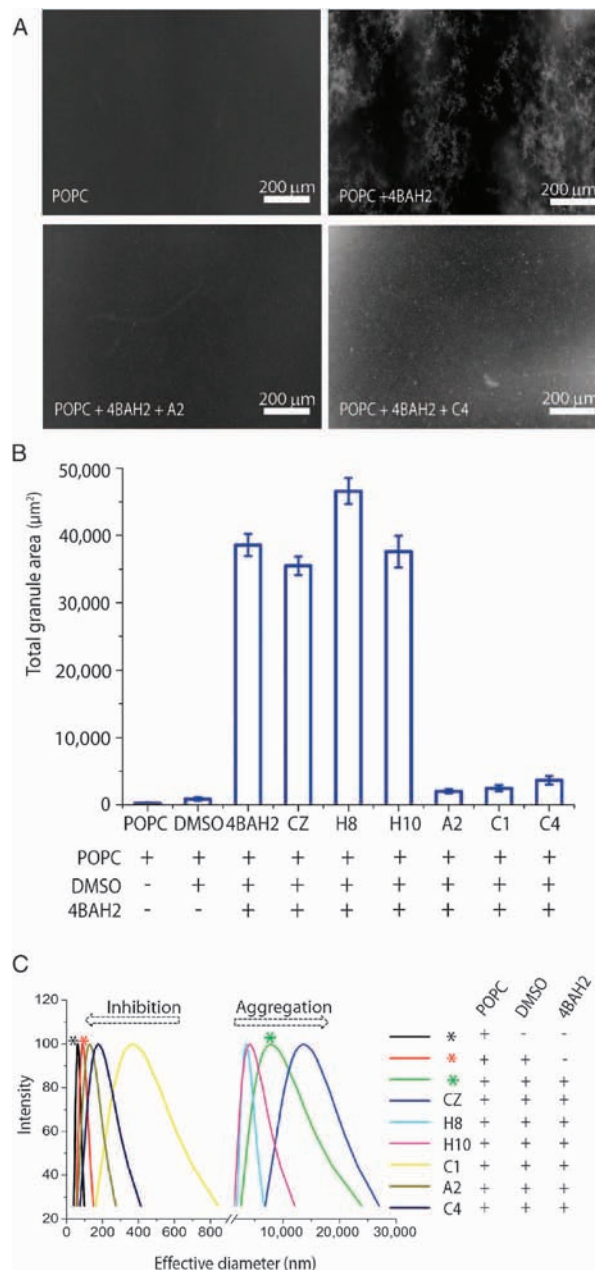


Fig. 4. Small-molecule compounds are identified that can inhibit 4BAH2-induced vesicle aggregation. (A) Fluorescence microscopy of 4BAH2-induced aggregation of lipid vesicles. Top row: POPC alone and POPC with 4BAH2. Bottom row: POPC with 4BAH2 and the A2 or C4 compounds. (B) The presence or absence of aggregates was analyzed in a high-throughput fashion with pattern recognition software based on total granule area of vesicle aggregation induced by 4BAH2. Data are presented as means ± SD (n = 3). (C) DLS assay (left panel) on selected candidate molecules identified to be positive in the HTS assay (and controls). Compounds assayed are shown at the right. Note that the black and red asterisks correspond to POPC lipid vesicles in buffer solution with (red) and without (black) DMSO and both in the absence of a candidate molecule. The green asterisk refers to the positive control of vesicles and 4BAH2 in buffer and DMSO solution in the absence of a candidate molecule. CZ [clemizole (18)], H8, and H10 were included as negative controls.

4BAH2 membrane association (Fig. 7F and fig. S12). C4 had a minor effect on the membrane association of 4BAH2 of either genotype (Fig. 7, E and F). The net effect of either C4 or A2, however, is to abrogate 4BAH2-mediated vesicle aggregation, a function that appears to be critical for the formation of the membranous web replication platform (fig. S13) and membrane-associated HCV RNA genome replication.

DISCUSSION

The limitations of current therapies for hepatitis C and the requirement for treatment cocktails to thwart the rapid development of multidrug resistance highlight the need for new classes of HCV drugs. Here, we tested a new target within the HCV NS4B protein, a conserved amphipathic helix essential for viral genome replication. This amphipathic helix, termed 4BAH2, displays a potential for self-oligomerization as well as the ability to promote the aggregation of lipid vesicles into macromolecular assemblies resembling key features of membranous webs—the HCV intracellular replication platform (12, 13). Furthermore, we used 4BAH2 vesicle aggregation-promoting activity to screen for candidate pharmacologic inhibitors. We showed that several such inhibitors could also alter HCV genome replication in a dose-dependent fashion. Moreover, the specificity of compounds for a particular HCV genotype could be predicted by their ability to inhibit 4BAH2 function based on AFM, QCM-D, and DLS assays. Detailed analysis of two compounds revealed that 4BAH2 function can be disrupted by either of two mechanisms: inhibition of 4BAH2 oligomerization or inhibi-

tion of the ability of 4BAH2 to associate with membranes. These results reveal a biochemical activity that may constitute a critical component of the mechanism of HCV's replication platform assembly and identify an anti-HCV strategy distinct from, and complementary to, other classes of drugs in development for hepatitis C.

Oligomerization of NS4B has been reported by others (25), but we found that specific point mutations within 4BAH2 that disrupted its amphipathic (Fig. 2A), but not helical (Fig. 2G), nature impaired the ability to oligomerize (fig. S14). Further, as shown in Figs. 1 and 2, 4BAH2 induces the aggregation of lipid vesicles and defines a heretofore unreported function within NS4B.

Our data suggest that 4BAH2-induced vesicle aggregation is also important for NS4B's role in the HCV life cycle. HCV replication is believed to occur in association with the membranous web (12, 13). Ectopic expression of NS4B alone has been reported to be sufficient for inducing membranous web formation (12). The relevant mechanism(s) whereby NS4B induces membranous webs is poorly understood. Although likely to involve multiple factors including ones supplied by the host cell, the 4BAH2 vesicle-aggregating activity reported here provides an attractive mechanism to account for some of the key elements of the previously described membranous web.

The mutation analysis of Fig. 3 represents a critical first step in the targeted development of new potential HCV therapeutics. However, target-specific assays must be developed, and understanding the mechanism of action of candidate inhibitors is needed, to efficiently translate such knowledge into new classes of HCV drugs.

One class of drugs now in advanced clinical development for hepatitis C is the NS5B polymerase inhibitors, where inhibition of NS5B function can be achieved by targeting NS5B both at the active site and at several epitopes distinct from the active site (26). Similarly, our study of how C4 and A2 inhibit 4BAH2 function suggests that the 4BAH2 class of inhibitors can inhibit HCV RNA genome replication, as well as a common target by an alternative mechanism, namely, by disrupting oligomerization or membrane association (see Fig. 6). Moreover, the above oligomeric model of 4BAH2 suggests the potential for transdominant inhibition of 4BAH2 function.

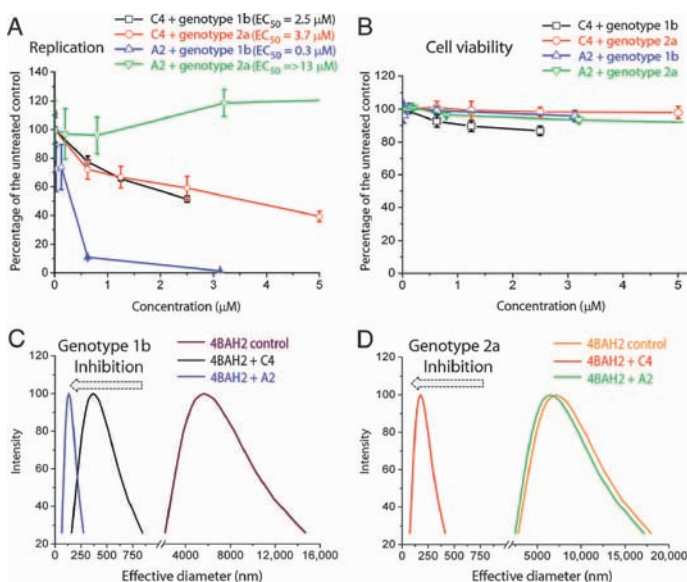


Fig. 5. HCV genome replication is inhibited by small-molecule inhibitors of 4BAH2 function in a genotype-specific manner. (A and B) Huh7.5 cells harboring genotype 1b replicon RNA (Bart791-luc) or full-length genotype 2a HCV RNA (J6/JFH-luc) were treated with various concentrations of C4 or A2 and assayed for (A) viral replication by luciferase activity ($n = 5$) and (B) cell viability ($n = 5$). (C and D) DLS assays of 4BAH2-induced vesicle aggregation were performed with genotype 1b 4BAH2 (C) or genotype 2a 4BAH2 (D) in the absence (control) or presence of either C4 or A2. Note that the x-axis scale is separated into two linear size ranges to directly compare the average vesicle size distribution in the presence or absence of compounds.

MATERIALS AND METHODS

Peptides

Peptides corresponding to the wild-type sequence of 4BAH2, as found in genotypes 1b (WRTLEAFWAKHMWNFISGIQYLA) and 2a (WPKVEQFWARHMWNFISGIQYLA), were commercially synthesized (Anaspec). For negative controls, three peptides harboring mutations in 4BAH2 (genotype 1b) were also synthesized. The sequences of the three different mutant peptides can be found in the Supplementary Material.

Small unilamellar vesicle preparation

Detailed methods are included in the Supplementary Material.

Plasmids

Detailed methods are included in the Supplementary Material.

Circular dichroism

Detailed methods are included in the Supplementary Material.

Quartz crystal microbalance with dissipation

Detailed methods are included in the Supplementary Material.

Dynamic light scattering

Detailed methods are included in the Supplementary Material.

Western blot analysis

Detailed methods are included in the Supplementary Material.

Production of the NS4B lentivirus and virus titer

Detailed methods are included in the Supplementary Material.

Atomic force microscopy

Detailed methods are included in the Supplementary Material.

High-throughput screen

To screen for compounds that inhibit 4BAH2-mediated aggregation of nano-sized vesicles, we performed a high-content imaging HTS (see fig. S6 for schematic). The assay was based on the ability of the 4BAH2 peptide to induce large-scale aggregation of fluorescently labeled vesicles that are readily detected by fluorescent microscopy. The fluorescent lipid vesicles were prepared as described above for small unilamellar vesicles, except for the addition of 0.05% Texas Red DHPE (molar ratio with POPC) during preparation of the lipid films.

A Caliper Life Sciences Sciclone ALH3000 liquid handler integrated system (Stanford University High-Throughput Bioscience Center) was used to accommodate 384-tip manifolds, enabling it to rapidly pipette volumes into 384-well microplates. The Z8 module that contains eight independent syringe-based pipettes, allowing liquid transfers with integrating a V&P Scientific 384 Pin Tool that is capable of 100-nl range transfers, was used (see the Supplementary Material for sequence details).

Transmission electron microscopy

Samples were fixed in 4% glutaraldehyde (Electron Microscopy Sciences) and 2% OsO₄, dehydrated in a series of ethanol washes, and infiltrated with EMbed 812 resin (Electron Microscopy Sciences) essentially as previously described (27). Center sections were stained in saturated uracetate and 0.2% lead citrate. Samples were ob-

served in a JEOL 1230 TEM at 80 kV, and images were taken with a Gatan MultiScan 791 digital camera (see the Supplementary Material for additional details).

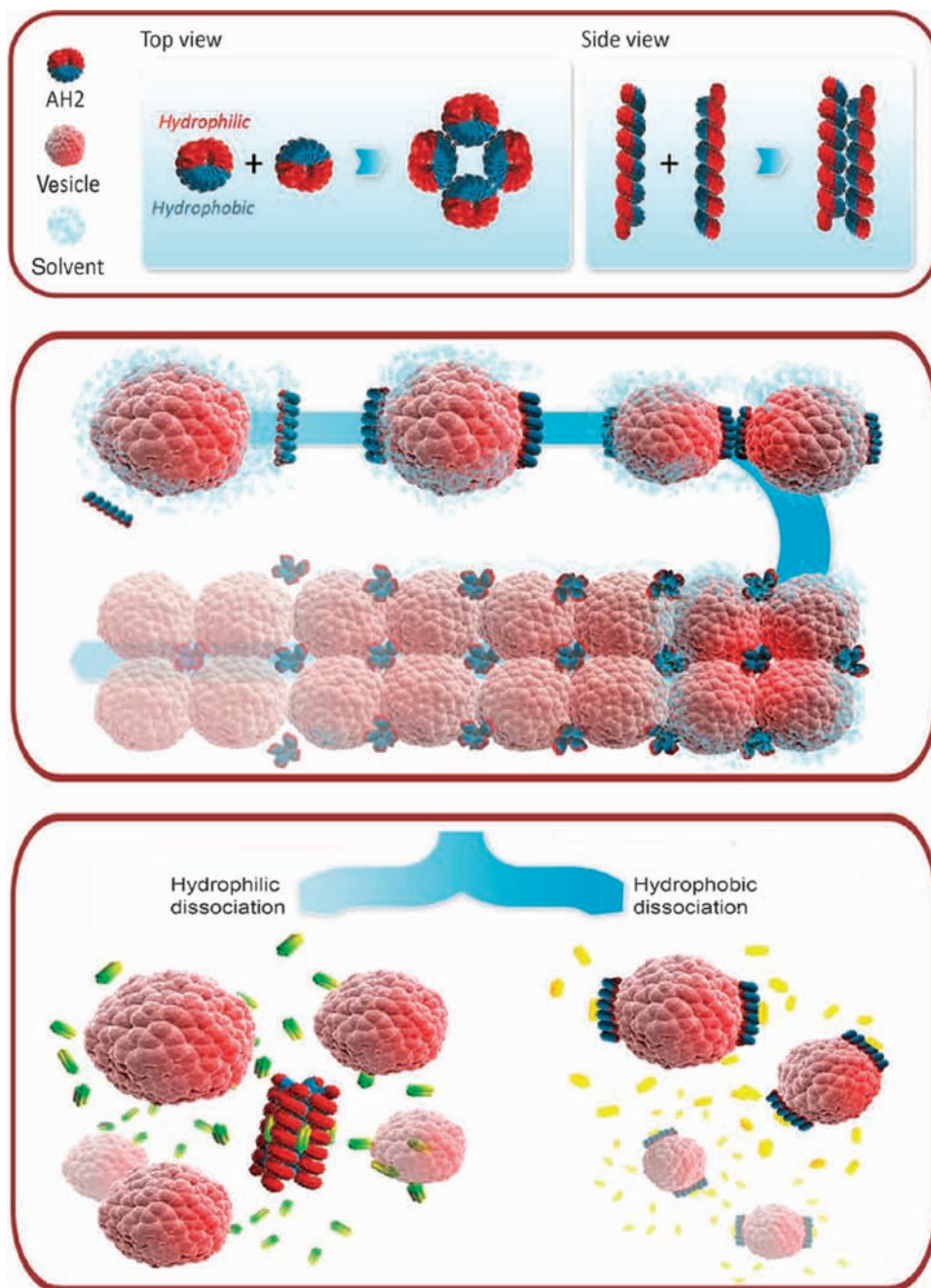


Fig. 6. Model of how 4BAH2 self-oligomerization and induction of lipid vesicle aggregation can be prevented by hydrophilic or hydrophobic dissociation. Top panel: 4BAH2 self-oligomerization is driven by hydrophobic interactions. Middle panel: Lipid vesicle aggregation is promoted by the interaction of the hydrophilic portions of 4BAH2 peptides with vesicles and the hydrophobic parts with each other. Bottom panel: Drug candidates inhibit 4BAH2-mediated lipid vesicle aggregation by either hydrophilic dissociation or hydrophobic dissociation. In the case of hydrophilic dissociation, the candidate drug (green and yellow molecules) interacts with the hydrophilic portion of 4BAH2 so that it inhibits 4BAH2 association with charged lipid head groups. For hydrophobic dissociation, different classes of drugs (schematized in yellow) interact with the hydrophobic portion of 4BAH2 to prevent peptide oligomerization, leading to abrogation of vesicle aggregation but not vesicle association of 4BAH2.

Colony formation assays

In vitro transcribed wild-type and mutant Bart791 RNAs (5 μg) were mixed with 6×10^6 Huh7 cells in RNase-free phosphate-buffered saline (PBS) (BioWhittaker) and transferred into a 2-mm-diameter gap cuvette (BTX). Electroporation was performed with a BTX model 830 electroporator, essentially as previously described (23). The electroporation condition was as follows: 680 V and five periods of 99 μs at 500-ms intervals. The electroporated cells were diluted in 30 ml of cell culture medium. Cells (300 μl) were transferred to 10-cm tissue culture dishes. At 24 hours after electroporation, cells were supplemented with untransfected feeder Huh7 cells to a final density of 10^6 per plate. After an additional 24 hours, the medium was supplemented with G418 to a final concentration of 750 $\mu\text{g}/\text{ml}$. This selection medium was replaced once every 3 days for 3 weeks. After selection, the plates were washed with PBS, incubated in 1% crystal violet in 20% ethanol for 5 min, and washed five times with water. Colonies on triplicate plates were counted and expressed as colonies per microgram electroporated RNA.

Transient replication assays

In vitro transcribed wild-type or mutant Bart791-luc RNAs (10 μg) were electroporated into Huh7 cells (23) as described above. The electroporated cells were diluted in 40 ml of cell culture medium. Cells (2 ml) were aliquoted in six-well tissue culture plates. Firefly luciferase activities were measured at 8, 48, 96, and 144 hours after electroporation with a firefly luciferase kit from Promega.

Antiviral assays of compounds

In vitro transcribed wild-type FL-J6/JFH-5'C19Rluc2Aubi and Bart791-luc RNAs were electroporated into Huh7.5 cells, essentially as previously described (23). Cells were seeded in 96-well plates. After 24 hours, individual test compounds (for example, C4 and A2) were added to the cells and media changes were performed daily with fresh aliquots of the same compounds. After 72 (for genotype 2a) or 110 (for genotype 1b) hours of treatment, cells were incubated for 2 hours at 37°C in the presence of 10% Alamar Blue reagent (TREK Diagnostic Systems) to assess cytotoxicity, followed by lysis and luciferase assays to assess for viral genome replication. Signal was normalized relative to untreated samples or samples grown in the presence of the corresponding concentration of dimethyl sulfoxide (DMSO). Experiments were repeated three times, each time with four replicates (see the Supplementary Material for additional details).

Infection and transfection expression

Infection and transfection were performed essentially as previously described (23). Briefly, a vaccinia virus that expresses the T7 RNA polymerase was used to infect Huh7 cells at a multiplicity of infection (MOI) of 10. After 45 min of incubation at 37°C, the cells were washed twice with Opti-MEM (Invitrogen) and subjected to transfection with pcDNA3.1-NS4B wild type or pcDNA3.1-NS4B-AH2 (M2) mutant. The cells were supplemented with growth media and incubated for 6 hours at 37°C, with about 80 to 90% of cells expressing the desired proteins confirmed by immunofluorescence analysis with a rabbit polyclonal antibody against NS4B.

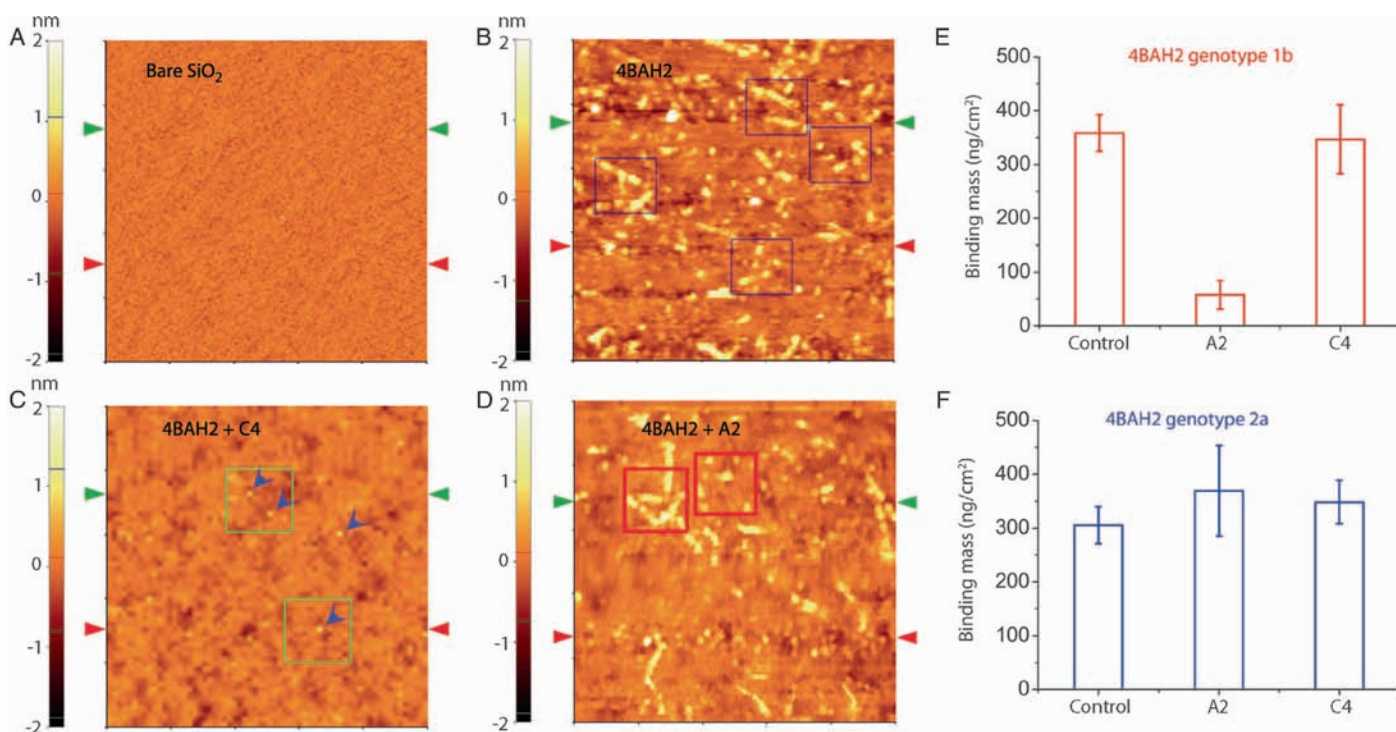


Fig. 7. Small-molecule inhibitors exhibit different effects on 4BAH2 inhibition. (A to D) AFM images were taken of bare SiO₂ substrate (A) and 4BAH2 aggregates on SiO₂ substrate after adsorption in the absence of compounds (B) or in the presence of C4 (C) or A2 (D). Original scan size, 5 × 5 μm [see fig. S10 for quantitative sample height analysis with line scans at

the level of two different arrowheads (red and green) and magnification at 5× of the indicated boxed areas]. (E and F) Binding mass of genotype 1b 4BAH2 (E) or genotype 2a 4BAH2 (F) to a SiO₂-supported POPC lipid bilayer platform in the presence or absence of A2 or C4, as determined by QCM-D monitoring (fig. S12).

Isolation of stable NS4B-expressing clone

Huh7.5 cells were infected with the concentrated NS4B lentiviruses at a MOI of 5 in the presence of polybrene (8 µg/ml, Sigma) and incubated at 37°C overnight. The following day, the infected cells were supplemented with growth media and incubated at 37°C for 4 days. On day 5 after infection, immunofluorescence analysis using a rabbit polyclonal antibody against NS4B was performed to confirm >98% of cells expressing the NS4B protein.

SUPPLEMENTARY MATERIAL

www.sciencetranslationalmedicine.org/cgi/content/full/2/15/15ra6/DC1
Materials and Methods

- Fig. S1. Protein secondary structures analysis.
Fig. S2. Far-ultraviolet CD recording of a synthetic 4BAH2 peptide.
Fig. S3. 4BAH2-induced vesicle aggregation by AFM.
Fig. S4. Mutant 4BAH2 peptides do not promote vesicle aggregation.
Fig. S5. Effect of 4BAH2 mutations on NS4B stability.
Fig. S6. Schematic of HTS.
Fig. S7. A 4BAH2 is conserved across all HCV genotypes and isolates.
Fig. S8. Molecular structures of C4 and A2.
Fig. S9. Identification of mutations conferring resistance to 4BAH2 pharmacologic inhibition.
Fig. S10. Quantitative sample height analysis with line scans and magnification of Fig. 7, A to D.
Fig. S11. Mutations in 4BAH2 completely abrogate 4BAH2 oligomerization.
Fig. S12. Small molecules have different effects on binding of 4BAH2 to biomimetic platform.
Fig. S13. Effects of an identified small-molecule inhibitor of 4BAH2 on membranous web formation.
Fig. S14. Mutations in 4BAH2 completely abrogate 4BAH2 oligomerization.

References

REFERENCES AND NOTES

- C. W. Shepard, L. Finelli, M. J. Alter, Global epidemiology of hepatitis C virus infection. *Lancet Infect. Dis.* **5**, 558–567 (2005).
- M. P. Manns, G. R. Foster, J. K. Rockstroh, S. Zeuzem, F. Zoulim, M. Houghton, The way forward in HCV treatment—finding the right path. *Nat. Rev. Drug Discov.* **6**, 991–1000 (2007).
- V. Soriano, M. G. Peters, S. Zeuzem, New therapies for hepatitis C virus infection. *Clin. Infect. Dis.* **48**, 313–320 (2009).
- B. D. Lindenbach, C. M. Rice, Unravelling hepatitis C virus replication from genome to function. *Nature* **436**, 933–938 (2005).
- D. Moradpour, F. Penin, C. M. Rice, Replication of hepatitis C virus. *Nat. Rev. Microbiol.* **5**, 453–463 (2007).
- K. Bienz, D. Egger, Y. Rasser, W. Bossart, Kinetics and location of poliovirus macromolecular synthesis in correlation to virus-induced cytopathology. *Virology* **100**, 390–399 (1980).
- P. W. Chu, E. G. Westaway, Molecular and ultrastructural analysis of heavy membrane fractions associated with the replication of Kunjin virus RNA. *Arch. Virol.* **125**, 177–191 (1992).
- L. H. Lazarus, R. Barzilai, Association of foot-and-mouth disease virus replicase with RNA template and cytoplasmic membranes. *J. Gen. Virol.* **23**, 213–218 (1974).
- C. M. Rice, in *Fields Virology*, B. N. Fields, D. M. Knipe, P. M. Howley, Eds. (Lippincott-Raven, Philadelphia, 1996), pp. 931–959.
- S. Froshauer, J. Kartenbeck, A. Helenius, Alphavirus RNA replicase is located on the cytoplasmic surface of endosomes and lysosomes. *J. Cell Biol.* **107**, 2075–2086 (1988).
- D. A. Suhy, T. H. Giddings Jr., K. Kirkegaard, Remodeling the endoplasmic reticulum by poliovirus infection and by individual viral proteins: An autophagy-like origin for virus-induced vesicles. *J. Virol.* **74**, 8953–8965 (2000).
- D. Egger, B. Wölk, R. Gosert, L. Bianchi, H. E. Blum, D. Moradpour, K. Bienz, Expression of hepatitis C virus proteins induces distinct membrane alterations including a candidate viral replication complex. *J. Virol.* **76**, 5974–5984 (2002).

- R. Gosert, D. Egger, V. Lohmann, R. Bartenschlager, H. E. Blum, K. Bienz, D. Moradpour, Identification of the hepatitis C virus RNA replication complex in Huh-7 cells harboring subgenomic replicons. *J. Virol.* **77**, 5487–5492 (2003).
- M. Elazar, P. Liu, C. M. Rice, J. S. Glenn, An N-terminal amphipathic helix in hepatitis C virus (HCV) NS4B mediates membrane association, correct localization of replication complex proteins, and HCV RNA replication. *J. Virol.* **78**, 11393–11400 (2004).
- T. Hügler, F. Fehrmann, E. Bieck, M. Kohara, H. G. Kräusslich, C. M. Rice, H. E. Blum, D. Moradpour, The hepatitis C virus nonstructural protein 4B is an integral endoplasmic reticulum membrane protein. *Virology* **284**, 70–81 (2001).
- M. Lundin, H. Lindström, C. Grönwall, M. A. Persson, Dual topology of the processed hepatitis C virus protein NS4B is influenced by the NS5A protein. *J. Gen. Virol.* **87**, 3263–3272 (2006).
- M. Lundin, M. Monné, A. Widell, G. Von Heijne, M. A. Persson, Topology of the membrane-associated hepatitis C virus protein NS4B. *J. Virol.* **77**, 5428–5438 (2003).
- S. Einav, D. Gerber, P. D. Bryson, E. H. Sklan, M. Elazar, S. J. Maerkl, J. S. Glenn, S. R. Quake, Discovery of a hepatitis C target and its pharmacological inhibitors by microfluidic affinity analysis. *Nat. Biotechnol.* **26**, 1019–1027 (2008).
- J. Gouttenoire, V. Castet, R. Montserret, N. Arora, V. Ruyschaert, E. Diesis, H. E. Blum, F. Penin, D. Moradpour, Identification of a novel determinant for membrane association in hepatitis C virus nonstructural protein 4B. *J. Virol.* **83**, 6257–6268 (2009).
- S. Ohki, Properties of lipid bilayer membranes. Determination of membrane thickness. *J. Theor. Biol.* **23**, 158–168 (1969).
- K. J. Blight, A. A. Kolykhalov, C. M. Rice, Efficient initiation of HCV RNA replication in cell culture. *Science* **290**, 1972–1974 (2000).
- E. H. Sklan, K. Staschke, T. M. Oakes, M. Elazar, M. Winters, B. Aroeti, T. Danieli, J. S. Glenn, A Rab-GAP TBC domain protein binds hepatitis C virus NS5A and mediates viral replication. *J. Virol.* **81**, 11096–11105 (2007).
- M. Elazar, K. H. Cheong, P. Liu, H. B. Greenberg, C. M. Rice, J. S. Glenn, Amphipathic helix-dependent localization of NS5A mediates hepatitis C virus RNA replication. *J. Virol.* **77**, 6055–6061 (2003).
- Stanford High-Throughput Bioscience Center; <http://htbc.stanford.edu>.
- G. Y. Yu, K. J. Lee, L. Gao, M. M. Lai, Palmitoylation and polymerization of hepatitis C virus NS4B protein. *J. Virol.* **80**, 6013–6023 (2006).
- P. L. Beaulieu, Recent advances in the development of NS5B polymerase inhibitors for the treatment of hepatitis C virus infection. *Expert Opin. Ther. Pat.* **19**, 145–164 (2009).
- T. Ushiki, Biological applications of electron microscopy. *Tanpakushitsu Kakusan Koso* **49**, 1714–1719 (2004).
- Acknowledgments: We thank the Stanford University High-Throughput Bioscience Center and Digestive Disease Center's Molecular Core; J. McLauchlan (MRC Virology Unit, Institute of Virology, Glasgow, UK) for the gift of polyclonal antibody against NS4B; and H. Greenberg, P. Sarnow, and R. Zare for kindly reading and thoughtful comments on the manuscript.
Funding: Burroughs Wellcome Fund Clinical Scientist Award in Translational Research (J.S.G.), NIH grants R01 DK066793 and R01AI087917, Stanford University Clinical and Translational Science Awards, and Stanford University SPARK Program. N.-J.C. is a recipient of an American Liver Foundation Postdoctoral Fellowship Award and a Global Roche Postdoctoral Fellowship. Author contributions: N.-J.C. conceived and designed the study, performed and analyzed experiments, and wrote the paper; H.D.-S., C.L., S.J.-C., P.B., and M.E. performed and analyzed experiments; M.M. and C.W.F. contributed to data analysis, and paper editing; J.S.G. conceived and designed the study, analyzed experiments, and wrote the paper.
Competing interests: A patent related to this work has been filed by Stanford University. N.-J.C., H.D.-S., C.L., and J.S.G. have an equity interest in Eiger BioPharmaceuticals Inc. J.S.G. is also a consultant to Eiger BioPharmaceuticals Inc.

Submitted 17 August 2009

Accepted 24 December 2009

Published 20 January 2010

10.1126/scitranslmed.3000331

Citation: N.-J. Cho, H. Dvory-Sobol, C. Lee, S.-J. Cho, P. Bryson, M. Masek, M. Elazar, C. W. Frank, J. S. Glenn, Identification of a class of HCV inhibitors directed against the nonstructural protein NS4B. *Sci. Transl. Med.* **2**, 15ra6 (2010).